



Article

Genome-Wide Identification, Molecular Characterization, and Involvement in Response to Abiotic and Biotic Stresses of the HSP70 Gene Family in Turbot (*Scophthalmus maximus*)

Weiwei Zheng^{1,2,†} , Xiwen Xu^{1,3,†}, Yadong Chen^{1,2,3}, Jing Wang², Tingting Zhang^{1,2}, Zechen E^{1,2}, Songlin Chen^{1,2,3,*} and Yingjie Liu^{2,4}

¹ Yellow Sea Fisheries Research Institute, Chinese Academy of Fishery Sciences, Qingdao 266071, China

² College of Fisheries and Life Science, Shanghai Ocean University, Shanghai 201306, China

³ Shandong Key Laboratory of Marine Fisheries Biotechnology and Genetic Breeding, Qingdao 266071, China

⁴ Chinese Academy of Fishery Sciences (CAFS), Beijing 100141, China

* Correspondence: chensl@ysfri.ac.cn

† These authors contributed equally to this work.

Abstract: Heat shock proteins 70 (HSP70s) are known to play essential roles in organisms' response mechanisms to various environmental stresses. However, no systematic identification and functional analysis has been conducted for HSP70s in the turbot (*Scophthalmus maximus*), a commercially important worldwide flatfish. Herein, 16 HSP70 genes unevenly distributed on nine chromosomes were identified in the turbot at the genome-wide level. Analyses of gene structure, motif composition, and phylogenetic relationships provided valuable data on the HSP70s regarding their evolution, classification, and functional diversity. Expression profiles of the HSP70 genes under five different stresses were investigated by examining multiple RNA-seq datasets. Results showed that 10, 6, 8, 10, and 9 HSP70 genes showed significantly up- or downregulated expression after heat-induced, salinity-induced, and *Enteromyxum scophthalmi*, *Vibrio anguillarum*, and Megalocytivirus infection-induced stress, respectively. Among them, *hsp70* (*hspa1a*), *hspa1b*, and *hspa5* showed significant responses to each kind of induced stress, and qPCR analyses further validated their involvement in comprehensive anti-stress, indicating their involvement in organisms' anti-stress mechanisms. These findings not only provide new insights into the biological function of HSP70s in turbot adapting to various environmental stresses, but also contribute to the development of molecular-based selective breeding programs for the production of stress-resistant turbot strains in the aquaculture industry.

Keywords: *Scophthalmus maximus*; heat shock protein 70 (HSP70); abiotic stress; biotic stress



Citation: Zheng, W.; Xu, X.; Chen, Y.; Wang, J.; Zhang, T.; E, Z.; Chen, S.; Liu, Y. Genome-Wide Identification, Molecular Characterization, and Involvement in Response to Abiotic and Biotic Stresses of the HSP70 Gene Family in Turbot (*Scophthalmus maximus*). *Int. J. Mol. Sci.* **2023**, *24*, 6025. <https://doi.org/10.3390/ijms24076025>

Academic Editor: Kiyoshi Naruse

Received: 22 February 2023

Revised: 19 March 2023

Accepted: 20 March 2023

Published: 23 March 2023



Copyright: © 2023 by the authors. Licensee MDPI, Basel, Switzerland. This article is an open access article distributed under the terms and conditions of the Creative Commons Attribution (CC BY) license (<https://creativecommons.org/licenses/by/4.0/>).

1. Introduction

Heat shock proteins (HSPs), first discovered in the salivary gland cells of the *Drosophila melanogaster* [1], are ubiquitously distributed in the cells of all organisms from bacteria to humans. HSPs are a large class of highly conserved molecular chaperons whose expression is induced by heat or other forms of stress [2]. Some of the HSP family members are known as housekeeping proteins that play distinct roles in the folding, assembling, secretion, intracellular localization, regulation, and degradation of proteins within unstressed cells. HSPs are generally classified into six distinct families, HSP110, HSP90, HSP70, HSP60, HSP40, and small HSPs, based on their molecular weight (MW) [3,4]. They are commonly present in the cytosol, mitochondria, endoplasmic reticulum, and nucleus [5]. Among all those in HSP families, HSP70 genes are the most evolutionarily conserved and have attracted considerable attention from researchers.

HSP70 genes contain three main conserved domains, a 40-kDa N-terminal ATPase domain (NBD) controlling the interaction with the client protein, an 18-kDa substrate-binding domain (SBD) that identifies the hydrophobic regions in a client protein during

the initial stages of client protein folding, and a 10-kD variable C-terminal domain [6,7]. Based on their functions and regulatory patterns, HSP70 genes are grouped into two distinct forms: constitutively expressed heat shock proteins (HSCs), which are present in cells under normal physiological conditions, and inducible heat shock proteins, which are expressed in response to specific stress conditions [8]. A substantial amount of evidence has suggested that HSP70 genes not only play crucial roles in promoting protein folding and proteostasis [4,9], the degradation of misfolded proteins [10], the membrane translocation of proteins [5], and the prevention of deleterious protein aggregation [11] and other cell-protective biological processes, but also exhibit essential functions in response to diverse environmental stresses (such as heat [12], hypoxia [13], pathogen infection [14], and heavy metal and organochlorine exposure [15]), physiological stress [16], and the immune response [17]. In summary, HSP70 genes are indispensable for maintaining protein homeostasis and cellular recovery after exposure to various environmental stresses.

Fish are generally exposed to various stresses in the water environment, such as cold or hot temperatures, hypoxia, low- or high-salinity stress, and other challenges caused by pathogen infection. Given the crucial functions of HSP70 genes in response to environmental stresses coupled with the great abundance of available genome sequence resources, an increasing number of HSP70 gene families have been identified at the genome-wide level in multiple teleosts, and the potential roles of these genes in response to abiotic and biotic stresses have also been described in recent years. For instance, 17 HSP70 genes were systematically characterized and analyzed in the spotted seabass (*Lateolabrax maculatus*); among them, 4, 11, and 7 gene family members were found to be involved in the response to heat, hypoxia, and alkalinity stress, respectively [18]. In the large yellow croaker (*Larimichthys crocea*), 17 HSP70 genes were identified at the genome-wide level; moreover, 6 gene family members were significantly up- or downregulated in liver tissue after exposure to cold and heat stresses, as determined with transcriptome data [19]. Moreover, a total of 20 HSP70 gene family members have been found in the *Boleophthalmus pectinirostris*, with most of these genes downregulated after exposure to high concentrations of ammonia [20]. Furthermore, 14 HSP70 genes have been detected in the *Cynoglossus semilaevis* through database searches and by manual selection, and expression profiles have demonstrated that most of these gene family members, especially *hspa5*, showed upregulated expression after exposure to low-salinity stress [21]. Moreover, a total of 16 HSP70 genes were detected in the genome of the rainbow trout (*Oncorhynchus mykiss*); in addition, an RNA-seq analysis indicated that 4 and 7 HSP70 gene family members showed significantly upregulated expression after heat stress in liver and head kidney tissues, respectively [22]. In the channel catfish (*Ictalurus punctatus*), 16 HSP70 genes were detected via a combination of genome databases and RNA-seq data, and 9 and 2 gene family members showed significant expression in gill tissue after a challenge with the *Flavobacterium columnare* and in intestine tissue after infection with the *Edwardsiella ictaluri* [14]. In the Japanese flounder (*Paralichthys olivaceus*), 15 HSP70 genes were identified, among which 5 gene family members were highly expressed post-infection with *Edwardsiella tarda* [23]. All of the above studies demonstrated that HSP70 genes play potentially important roles in the biological mechanisms underlying the responses to biotic and abiotic stresses in teleosts. However, no systematic identification or functional analysis of the HSP70 gene family has been performed in the turbot to date.

The turbot (*Scophthalmus maximus*, FishBase ID: 1348) is an economically important cold-water flatfish species native to the Northeast Atlantic [24]. Due to its tasty meat and high nutritional value, the turbot has become the marine flatfish produced at the highest level under aquaculture conditions worldwide [25]. Unfortunately, due to high-density industrial farming coupled with an increased frequency in extreme weather events, in recent years, the turbot has faced a variety of abiotic and biotic stresses during aquaculture, such as heat stress induced by global warming [26], salinity stress caused by disrupted climate conditions and tidal water flow [27,28], as well as pathogen-induced stresses resulting from high-density industrial farming [29–32]. These environmental stresses severely threatened the welfare or caused elevated mortality in this species under aquaculture con-

ditions, leading to huge economic losses that greatly impede the healthy and sustainable development of the turbot industry. Because of the essential functions of HSP70 genes in response to diverse stresses, systematically identifying and exploring their expression patterns under abiotic and biotic stresses is expected to be valuable for further functional studies and exhibit important practical significance in the development of efficient farming practices, thereby leading to an increase in turbot fitness in aquaculture production. Fortunately, high-quality genome assembly [33] and multiple published RNA-seq datasets resources [26–28,30–32,34,35] made available in recent years make it possible to perform systematic identification, phylogenetic analysis, and a functional study of HSP70 genes in the turbot.

In the present study, a complete set of HSP70 genes in the turbot was first identified at the genome-wide level. Molecular characterizations, including biochemical properties, protein structure, and molecular evolution, were also determined. Furthermore, evolutionary relationship, exon–intron structure, and conserved domain and motif analyses were carried out, respectively. In addition, to better understand the role of HSP70 genes challenged by a variety of environmental stresses in the turbot, the gene expression patterns in distinct tissues after exposure to diverse abiotic and biotic stresses, such as heat, salinity, and three different pathogen infection stresses, were investigated by analyzing multiple stress-related RNA-seq datasets. Finally, qPCR analyses were performed to further validate the functions of the HSP70 gene candidates that showed comprehensive anti-stress responses to both abiotic and biotic stresses, as determined by the results of RNA-seq data analyses. This may be the first systematic identification and functional investigation of HSP70 genes in the turbot. The findings of this study will aid in the study of the molecular regulatory mechanism of HSP70 genes in response to environmental stresses and provide new insight into increasing the environmental adaptation and comprehensive stress resistance of the turbot.

2. Results

2.1. Identification and Characteristics of HSP70 Genes in Turbot

In the present study, a total of 16 HSP70 genes were identified in the turbot at the genome-wide level using a combination of BLASTp and HMM searches and confirmation with an NCBI CDD scan. Then, turbot HSP70 genes were named following the nomenclature of *D. rerio* heat shock proteins. Information on the domains of turbot HSP70 genes is shown in Table 1 and Supplementary Materials Table S1. Comparisons of the numbers of HSP70 genes in humans and other well-characterized teleosts are shown in Table S2, indicating their high evolutionary conservation among species. In addition, the basic physicochemical properties of proteins encoded by HSP70 genes in the turbot are shown in Tables 1 and S3. Specifically, the number of amino acids varied from 431 (*hspa8a.1*) to 986 (*hyou1*). The predicted molecular weights (MWs) ranged from 48.13 kDa (*hspa8a.1*) to 110.91 kDa (*hyou1*), and the theoretical isoelectric point (pI) ranged from 5.00 (*hspa5*) to 8.48 (*hspa12b*). Furthermore, *hspa12b* showed the longest conserved domain at 497 amino acids, whereas the shortest domain was found in *hspa8a.1* (315 amino acids). Moreover, the grand average of hydropathicity (GRAVY) values of turbot HSP70 proteins were all negative, indicating that all the proteins were hydrophobic. Moreover, the prediction of the protein instability index (II) (a reference value for protein stability in vitro analysis) showed that 7 of the 16 HSP70 proteins were identified as stable proteins (II < 40), with the others predicted to be unstable (II > 40). Investigation of the molecular properties of HSP70 proteins aids in determining their biological functions.

Table 1. Summary of sequence characteristics of HSP70 genes in *S. maximus*.

Group	Gene Name	Chr	Gene Length (bp)	Numbers of Amino Acids	MW (Da)	pI	Domain	Domain Location (aa)
hspa1	<i>hspa1b</i>	Chr3	2780	638	70,307.59	5.42	HSPA1-2_6-8-like_NBD	8-383
	<i>hsp70</i> (<i>hspa1a</i>)	Chr17	2464	639	70,233.30	5.44	HSPA1-2_6-8-like_NBD	8-383
hspa4	<i>hspa4a</i>	Chr2	14,103	810	90,727.11	5.3	HSPA4_NBD	2-384
	<i>hspa4b</i>	Chr9	8098	845	94,849.45	5.04	HSPA4_NBD	2-384
	<i>hspa4l</i>	Chr15	8780	832	93,131.57	5.35	HSPA4_NBD	2-384
hspa5	<i>hspa5</i>	Chr20	3922	654	72,220.73	5.0	HSPA5-like_NBD	26-401
	<i>hspa8a.1</i>	Chr2	2990	431	48,133.63	6.87	HSPA1-2_6-8-like_NBD	52-367
hspa8	<i>hspa8a.2</i>	Chr2	4781	651	71,225.32	5.26	HSPA1-2_6-8-like_NBD	6-381
	<i>hspa8b</i>	Chr11	4378	646	70,684.97	5.36	HSPA1-2_6-8-like_NBD	6-381
	<i>hsc70</i>	Chr1	4665	653	71,324.65	5.27	HSPA1-2_6-8-like_NBD	6-381
hspa9	<i>hspa9</i>	Chr9	8965	685	74,100.10	6.09	HSPA9-like_NBD	52-428
hspa12	<i>hspa12a</i>	Chr10	28,355	670	74,993.54	6.57	HSPA12A_like_NBD	54-520
	<i>hspa12b</i>	Chr2	15,095	715	79,467.95	8.48	HSPA12B_like_NBD	57-554
hspa13	<i>hspa13</i>	Chr11	4707	439	47,641.75	5.91	HSPA13-like_NBD	23-431
hspa14	<i>hspa14</i>	Chr2	8663	506	54,385.87	5.99	HSPA14-like_NBD	2-376
hyou1	<i>hyou1</i>	Chr2	18,128	986	110,913.87	5.01	HYOU1-like_NBD	30-416

2.2. Phylogenetic Analysis of HSP70 Genes among Teleost Species

To clarify the phylogenetic relationships and the classification of HSP70 genes among different teleost species, an unrooted NJ phylogenetic tree was constructed using HSP70 protein sequences from the turbot and three other representative teleost species (Table S4). As shown in Figure 1, 66 HSP70 genes were classified into nine distinct groups, the hspa1, hspa4, hspa5, hspa8, hspa9, hspa12, hspa13, hspa14, and hyou1 groups. All of the turbot HSP70 genes were classified into these nine different clades, and they were first grouped with orthologous genes of selected species with strong bootstrap values. In addition, two genes (*hspa1b* and *hsp70*), two genes (*hspa12a* and *hspa12b*), three genes (*hspa4a*, *hspa4b*, and *hspa4l*), and four genes (*hspa8a.1*, *hspa8a.2*, *hspa8b*, and *hsc70*) were identified as duplicated turbot HSP70 genes in the hspa1, hspa12, hspa4, and hspa8 groups, respectively. In contrast, no gene duplications were found in the hspa5, hspa9, hspa13, hspa14, or hyou1 groups, which was similar to the results obtained in an analysis of three other teleost species.

2.3. Chromosomal Distribution and Selection Test of Duplicated HSP70 Genes

Sixteen HSP70 genes were unevenly distributed on nine turbot chromosomes (Figure 2). Specifically, six HSP70 genes, *hspa8a.1*, *hspa8a.2*, *hspa4a*, *hspa12b*, *hspa14*, and *hyou1*, were located on Chr2. In addition, two HSP70 genes were observed on Chr 9 and Chr 11. In addition, the remaining six HSP70 genes were distributed on different chromosomes, such as Chr 1, Chr 3, Chr 10, Chr 15, Chr 17, and Chr 20. In terms of duplicated genes, *hspa8a.1* and *hspa8a.2* were located on the same chromosome, while the other duplicated gene pairs were located on different chromosomes. To investigate whether these duplicated HSP70 genes experienced various selection pressures, the nonsynonymous (K_a), synonymous (K_s), and K_a/K_s ratios for all duplicated HSP70 gene pairs were calculated (Table 2). The results showed that the K_a/K_s ratios of all the duplicated HSP70 gene pairs ranged from 0.04777 to 0.2558, which were much lower than 1.0, indicating that they had all been subjected to purifying selection.

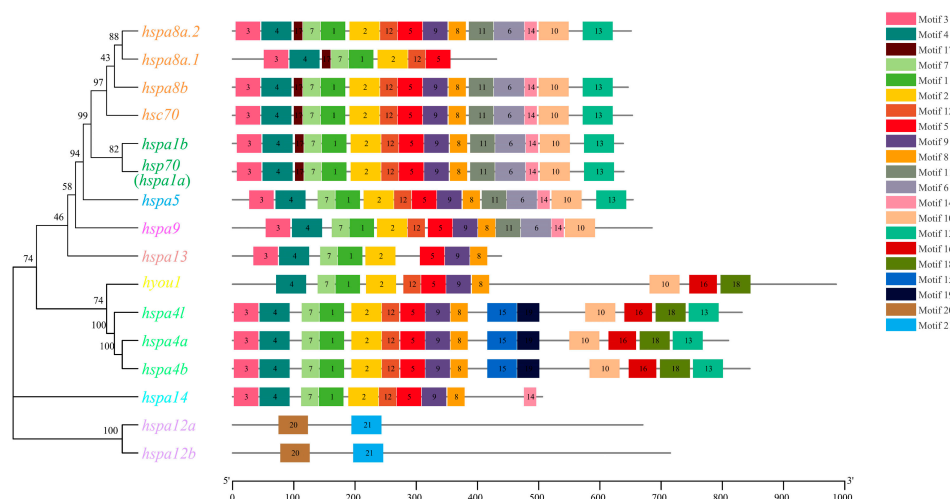


Figure 4. The combination of phylogenetic relationship and conserved motifs. The left of the graph shows the phylogenetic relationships of *S. maximus* HSP70 genes. The right of the graph shows the distribution of conserved motifs and each colored rectangular box represents a motif.

2.5. Subcellular Localization and Protein Structure Analysis

The prediction of subcellular localization indicated that most HSP70 proteins in the turbot were located in the cytosol and extracellular space; however, the proteins encoded by *hspa9*, *hspa12b*, and *hyou1* were localized in the mitochondria, nucleus, and endoplasmic reticulum, respectively (Table 3). Moreover, the secondary structure prediction showed that turbot HSP70 proteins were primarily composed of alpha helices (32.39–50.51%) and random coils (29.61–44.48%), while extended strands and beta turns accounted for 12.37–23.72% and 3.31–7.37% of the structure, respectively (Table 3). In addition, the signal peptide prediction results demonstrated that only *hyou1* and *hspa5* encoded proteins with Sec/SPI signal peptides with SP values of 0.995566 and 0.999579, respectively, and these gene products were preliminarily identified as secretory proteins. As shown in Figure 5, the cleavage site was between positions 27 and 28 with a marginal probability of 0.636974 in *hyou1*, while in *hspa5* the cleavage site was between positions 16 and 17 with a marginal probability of 0.982612.

Table 3. The secondary structure prediction and subcellular location prediction of HSP70 proteins in *S. maximus*.

Gene Name	Alpha Helix	Extended Strand	Beta Turn	Random Coil	Subcellular Location
<i>hspa4b</i>	43.55%	13.61%	3.31%	39.53%	cytosol
<i>hspa4a</i>	44.32%	14.20%	3.70%	37.78%	cytosol
<i>hspa4l</i>	43.87%	13.82%	3.73%	38.58%	cytosol
<i>hyou1</i>	50.51%	12.37%	3.75%	33.37%	cytosol
<i>hspa12a</i>	32.39%	19.10%	4.03%	44.48%	cytosol
<i>hspa8a.1</i>	41.76%	20.19%	5.10%	32.95%	extracellular
<i>hspa12b</i>	32.73%	19.02%	5.31%	42.94%	cytosol
<i>hspa13</i>	42.60%	21.18%	6.61%	29.61%	cytosol
<i>hsp70 (hspa1a)</i>	41.78%	18.94%	6.73%	32.55%	cytosol
<i>hspa8a.2</i>	41.32%	18.13%	6.76%	33.79%	cytosol
<i>hspa9</i>	41.61%	19.56%	6.86%	31.97%	mitochondrial
<i>hspa14</i>	37.55%	23.72%	6.92%	31.82%	cytosol
<i>hsc70</i>	41.50%	18.22%	7.04%	33.23%	nuclear
<i>hspa5</i>	44.04%	18.35%	7.19%	30.43%	extracellular
<i>hspa8b</i>	42.41%	17.96%	7.28%	32.35%	cytosol
<i>hspa1b</i>	43.10%	18.50%	7.37%	31.03%	endoplasmic reticulum

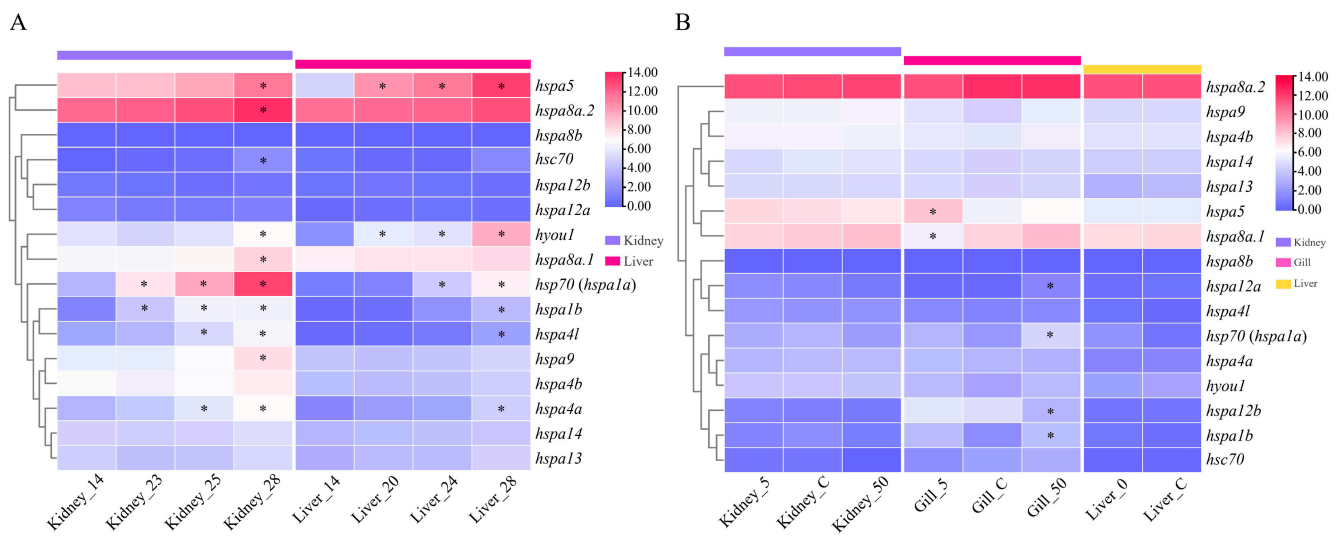


Figure 6. Expression patterns of HSP70 genes under abiotic stresses in *S. maximus*. (A) Expression patterns of HSP70 genes in kidney and liver tissues under heat stress. Control group: 14, 14 °C; 20, 23, 24, 25, and 28 represent 20 °C, 23 °C, 24 °C, 25 °C, and 28 °C heat stress groups, respectively. (B) Expression patterns of HSP70 genes in kidney, gill, and liver tissues under salinity stress. C: 30‰ (natural seawater); 50: 50‰; 5: 5‰; 0: 0‰ (fresh water). Cells with different colors correspond to different expression levels, which were normalized into $\log_2(\text{TPM} + 1)$. * indicates differentially expressed (or significantly up- or downregulated) HSP70 genes with $|\log_2\text{fold change (FC)}| > 1$ and false discovery rate (FDR) < 0.01 .

In a word, four HSP70 genes, *hsp70 (hsa1a)*, *hspa1b*, *hspa5*, and *hspa8a.1*, were significantly induced both by heat and salinity stresses, indicating their essential roles in response mechanisms to various abiotic stresses in turbot.

2.7. Expression Patterns of HSP70 Genes under Biotic Stresses

Using pathogen (parasite, bacteria, and virus)-challenged RNA-Seq datasets, the expression profiles of turbot HSP70 genes in different tissues under biotic stress were determined (Figure 7). The detailed expression data are provided in Table S7. After parasite (*E. scophthalmi*) infection, eight DE HSP70 genes (*hsp70 (hsa1a)*, *hspa4a*, *hsc70*, *hspa1b*, *hspa9*, *hspa8b*, *hspa4l*, and *hspa5*) identified in four distinct tissues showed different expression than in the healthy group. Specifically, in the kidney, *hsp70 (hsa1a)* and *hspa4a* were upregulated both at 24 and 42 days post-infection (dpi) with *E. scophthalmi*. In the pyloric caeca, *hsc70*, *hsp70 (hsa1a)*, *hspa1b*, *hspa4a*, and *hspa9* were all upregulated at 42 dpi, while no DE HSP70 genes were found at 24 dpi. In addition, no DE HSP70 genes were detected in the spleen. In the thymus, only the expression of *hspa8b* was detected significantly upregulated at 42 dpi. Moreover, in the blood with four different levels (incipient, slight, moderate, and severe) of *E. scophthalmi* infection, DE HSP70 genes, including *hspa4l* and *hspa5*, were found only in the severely infected group, and they all had upregulated expression.

Following bacterial (*V. anguillarum*) challenge, 10 DE HSP70 genes, *hsp70 (hsa1a)*, *hspa13*, *hspa1b*, *hspa4a*, *hspa4b*, *hspa4l*, *hspa5*, *hspa9*, *hyou1*, and *hspa12b*, were detected in five different tissues compared to the control group. Specifically, in the intestine, three DE HSP70 genes, *hsp70 (hsa1a)*, *hspa4a*, and *hspa5*, were all upregulated at 1 h after challenging with *V. anguillarum* and then were downregulated continuously at 4 h and 12 h. In the spleen, no DE HSP70 genes were identified. In addition, *hsp70 (hsa1a)*, *hspa1b*, and *hspa12b* were differentially expressed in the gill, and among these genes, the expression of *hsp70 (hsa1a)* and *hspa1b* was upregulated, while that of *hspa12b* was downregulated. Furthermore, in the kidney, two DE HSP70 genes, *hsp70 (hsa1a)* and *hspa4l*, had significantly upregulated expression. Moreover, seven DE HSP70 genes, *hspa4a*, *hyou1*, *hspa5*, *hspa13*, *hspa9*, *hspa4b*, and *hsp70 (hsa1a)*, had upregulated expression in the liver.

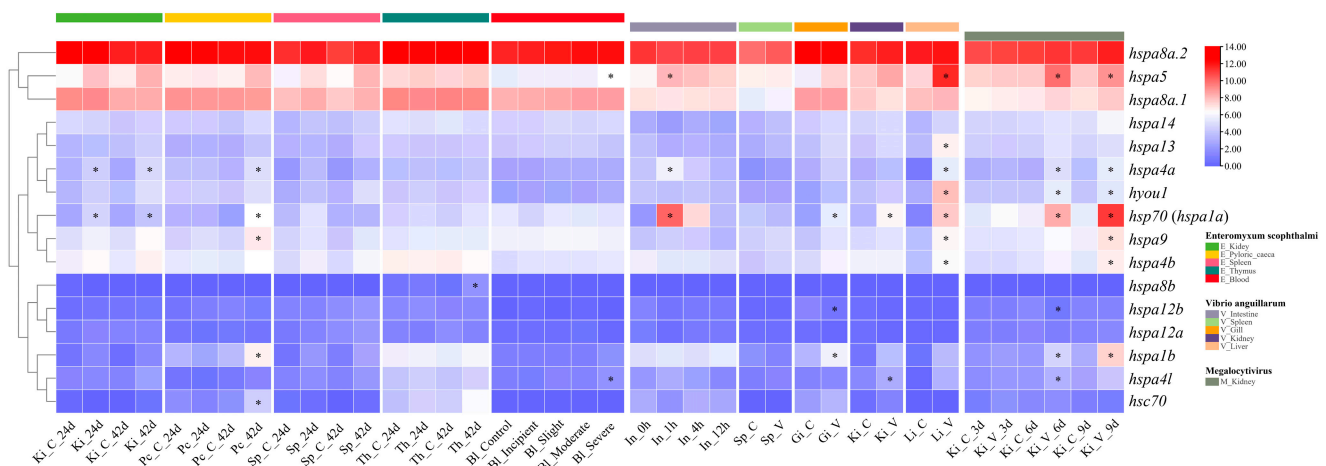


Figure 7. Heat map of HSP70 genes expression in *S. maximus* under pathogens (*E. scophthalmi*, *V. anguillarum*, Megalocytivirus) infection. Ki, Pc, Sp, Th, Bl, In, Gi, and Li represent kidney, pyloric caeca, spleen, thymus, blood, intestine, gill, and liver, respectively. C represents control group, V represents *V. anguillarum* infection, M represents Megalocytivirus infection. Cells with different colors correspond to different expression levels, which were normalized into $\log_2(\text{TPM} + 1)$. * indicates the differentially expressed (or significantly up- or downregulated) HSP70 genes with $|\log_2\text{FC}| > 1$ and $\text{FDR} < 0.01$.

After infection with a virus (*Megalocytivirus*), a total of nine DE HSP70 genes, *hsp70* (*hspa1a*), *hspa12b*, *hspa1b*, *hspa4a*, *hspa4b*, *hspa4l*, *hspa5*, *hspa9*, and *hyou1*, were detected in the head kidney. In detail, at 3 dpi, no DE HSP70 genes were found. By comparison, *hsp70* (*hspa1a*), *hspa1b*, *hspa5*, *hspa4a*, *hyou1*, *hspa4l*, and *hspa12b* were differentially expressed at 6 dpi, and they were all upregulated except for *hspa12b*, which showed downregulated expression. In addition, the DE HSP70 genes identified at 9 dpi, including *hsp70* (*hspa1a*), *hspa4b*, *hspa9*, *hspa4l*, *hyou1*, *hspa4a*, *hspa5*, and *hspa1b*, all had upregulated expression.

In summary, a total of six HSP70 genes, *hsp70* (*hspa1a*), *hspa1b*, *hspa4a*, *hspa4l*, *hspa5*, and *hspa9*, were significantly affected by three different pathogens, demonstrating their essential roles in response to various biotic stresses.

2.8. qPCR Validation of HSP70 Gene Candidates Involved in Comprehensive Anti-Stress Responses

Based on the expression pattern analysis of HSP70 genes under both biotic and abiotic stresses determined using RNA-seq datasets, we concluded that *hsp70* (*hspa1a*), *hspa1b*, and *hspa5* may be the HSP70 gene family members with comprehensive anti-stress functions. To further validate their potential comprehensive anti-stress functions, qPCR analyses were conducted. We first validated the expression patterns of *hsp70* (*hspa1a*), *hspa1b*, and *hspa5* in the liver and kidney tissues of the turbot at 24 h after heat stress (Figure 8A,B). The results showed that *hsp70* (*hspa1a*), *hspa1b*, and *hspa5* exhibited similar expression patterns, that is, an extremely significant upregulation in expression continuously as the temperature increased in the liver and kidney tissues after heat stress. This finding was consistent with the results of the RNA-seq analysis, indicating that *hsp70* (*hspa1a*), *hspa1b*, and *hspa5* do play important roles in response to abiotic stress, especially heat stress. We then also systematically illustrated the expression patterns of *hsp70* (*hspa1a*), *hspa1b*, and *hspa5* in the kidney and spleen tissues of the turbot at 0, 6, 12, 24, and 48 h after infection with *E. tarda* using qPCR (Figure 9). The results showed that *hsp70* (*hspa1a*), *hspa1b*, and *hspa5* were all significantly or extremely significantly upregulated in the spleen and kidney tissues at 6, 12, 24, and 48 h post-infection with *E. tarda*, especially *hsp70* (*hspa1a*) and *hspa1b*, indicating their crucial roles in response to biotic stress.

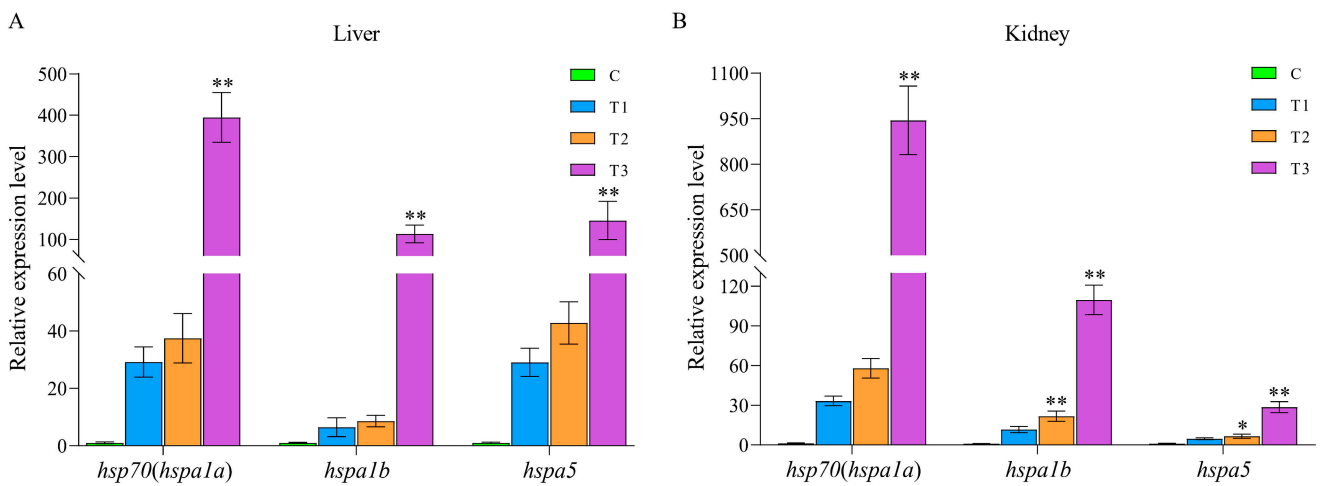


Figure 8. The validation of expression patterns of *hsp70* (*hspa1a*), *hspa1b*, and *hspa5* in liver (A) and kidney (B) tissues at 24 h after heat stress. The mRNA expression levels were determined by qPCR analysis using the $2^{-\Delta\Delta C_t}$ method. C, T1, T2, and T3 represent 18 °C, 22 °C, 26 °C, and 30 °C heat treatment groups, respectively. * and ** indicate the significant differences at $p < 0.05$ and $p < 0.01$ between the control (C) and heat treatment groups (T1, T2, and T3), respectively.

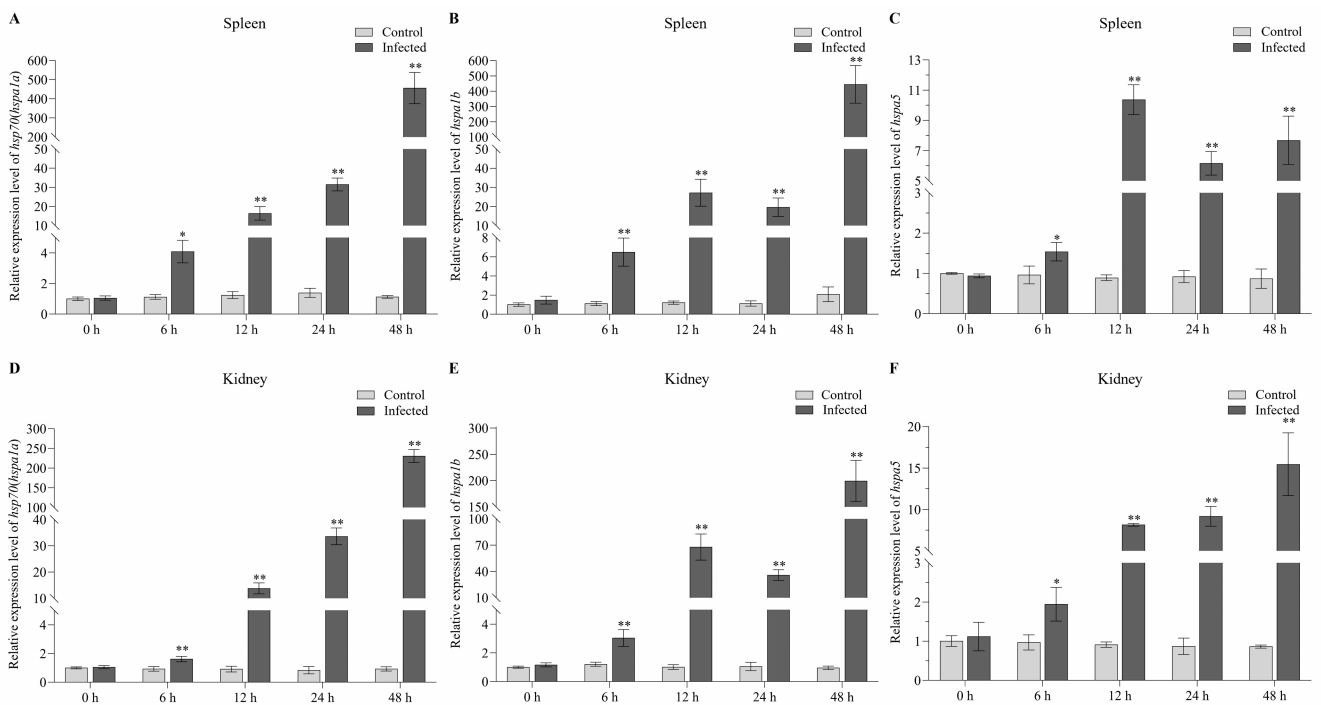


Figure 9. The validation of expression patterns of *hsp70* (*hspa1a*), *hspa1b*, and *hspa5* in spleen (A–C) and kidney (D–F) tissues at 0, 6, 12, 24, and 48 h post-infection with *E. tarda*. The mRNA expression levels were determined by qPCR analysis using the $2^{-\Delta\Delta C_t}$ method. * and ** indicate the significant differences at $p < 0.05$ and $p < 0.01$ between the control and infected groups at the same time, respectively.

3. Discussion

Heat shock protein 70 (HSP70) gene family members are involved in various house-keeping and stress-related activities in all organisms from bacteria to mammals [36,37]. Due to their important roles, especially in enhancing the response of cells to various stress stimuli, the HSP70 gene family has been extensively studied in a variety of aquaculture species, including invertebrate [38], bivalve [39], and multiple teleost species [14,18–21,23].

Nevertheless, a systematic analysis of HSP70 genes in the turbot has been lacking. In the present study, we conducted comprehensive research on the HSP70 gene family in the turbot, including the systematic identification of genes at the genome-wide level and analysis of biochemical characteristics, phylogeny, gene structure, and conserved motifs. In addition, to determine the involvement of these genes in mechanisms associated with responses to abiotic and biotic stresses, the expression patterns of HSP70 genes in the turbot under heat-induced, salinity-induced, and parasitic, bacterial, and virus infection-induced stresses were determined by examining multiple RNA-seq datasets. Importantly, qPCR was performed to further verify the potential functions of the HSP70 gene candidates showing comprehensive anti-stress in response to both biotic and abiotic stresses.

In the present study, a total of 16 HSP70 genes were detected in the turbot, which was more than the number previously found in crustaceans (*Portunus trituberculatus*) (9) [40] but considerably less than the number found in bivalve species, such as the *Crassostrea gigas* (88) [41], *Mercenaria mercenaria* (133) [39], and *Cyclina sinensis* (60) [39], and similar to the number in humans (17) [42] and in other teleost species (14–20). Although the number of HSP70 genes varies among species, they display high-level evolutionary conservation in humans and teleost species. The differences in gene number might be a result of gene duplication or gene loss during the process of evolution. In addition, the turbot contained almost all the orthologs of HSP70 genes in zebrafish and other teleosts, with the exception of *hsph1*, for which an ortholog has been found only in zebrafish, not other teleost species. We speculated that *hsph1* might have been lost from the genome of most teleosts during evolution. Furthermore, the phylogenetic analysis of four representative teleost species showed that the HSP70 genes within the same group were more similar to each other than to those in other groups, demonstrating that HSP70 genes were highly conserved during teleost evolution.

Gene duplication represents the principal mechanism by which gene families expand and provides raw materials for the evolution of novel gene functions [43–45]. In this study, we observed that duplicated HSP70 genes were mainly contained in the hapa1, 4, 8, and 12 groups in all teleosts. In the turbot, the genes *hspa8a.1* and *hspa8a.2* located on Chr 2 were identified in tandem duplications [46], whereas other genes were distributed on different chromosomes, indicating that whole-genome duplication and tandem duplication events both contributed to the evolution and expansion of HSP70 genes in the turbot. Classic examples of gene family expansion have been found in bivalves; for example, 88 HSP70 gene copies have been identified in the *C. gigas* [41], and 133 copies have been identified in the *M. mercenaria* [39]. Studies on bivalves have demonstrated that the expansion of HSP70 genes was probably crucial to the environmental adaptation process in the highly stressful intertidal zone [39,41]. In our study, duplicated genes, that is, *hsp70* (*hspa1a*) and *hspa1b*, were differentially expressed under five stress conditions (heat-, salinity-, and parasitic, bacterial, and virus infection-related stress conditions). Moreover, the expansion of *hspa1* might have contributed to the terrestrial adaptations in *B. pectinirostris*, which enabled them to spend a considerable part of their lives on land, during evolution [20]. In addition, the *Ka/Ks* ratios of all repetitive HSP70 gene pairs in the turbot were significantly less than 1 (varying from 0.047773 to 0.255827), indicating that repeated genes in the turbot underwent a strong purifying selection during evolution.

Gene structure provides strong support for evolutionary classifications within a gene family [47]. Herein, a combination of the results from phylogenetic analysis and gene structure analysis showed that paralogous gene pairs, that is, HSP70 genes derived from the same group, showed highly similar exon–intron distribution patterns and a conserved motif constitution, demonstrating their high evolutionary conservation and similar functions within a group. In addition, numerous studies have proven that distinct exon–intron structures and motif patterns in HSP70 genes are related to their unique biological functions [19,48,49]. In the turbot, the numbers of exons (ranging from 2 to 25) and motifs (ranging from 2 to 21) varied considerably between groups, indicating their potential biological function diversification among members in diverse groups. Interestingly, *hsp70*

(*hspa1a*) and *hspa1b*, each with only one intron and two exons, were significantly induced by all five evaluated stress conditions, which might have been due to the low number of introns and exons, allowing efficient transcription.

To detect the involvement of HSP70 genes in abiotic stress, the expression profiles of HSP70 genes after turbot were challenged by heat and salinity stresses were illustrated for the first time. Under heat stress treatment, 10 and 6 DE HSP70 genes were detected in the kidney and liver, respectively. With increasing temperature, almost all of these genes had significantly and continuously upregulated expression, and the number of DE HSP70 genes was clearly increased. Similar results have also been found in the *L. maculatus* and *O. mykiss*, in which most of the examined HSP70 genes showed significantly upregulated expression in different tissues after exposure to heat stress [18,22]. Moreover, four significantly upregulated HSP70 genes in both kidney and liver tissues were identified, *hsp70* (*hspa1a*), *hspa1b*, *hspa5*, and *hspa8a.1*. Among these genes, *hsp70* (*hspa1a*) was one of the most intense responsive genes in the liver, muscle, and gill tissues after heat stress in the spotted seabass [18]. Furthermore, the expression of *hsp70* (*hspa1a*), *hspa5*, and *hspa8a* was also significantly increased both in the liver and head kidney of the rainbow trout after heat treatment (24 °C) [22] demonstrating their essential roles in heat stress responses, indicating that these genes might be selected as biomarkers of heat stress. In contrast to the highly inducible expression of more than one half of the HSP70 genes expressed after exposure to heat stress, only four HSP70 genes showed significantly upregulated expression in all tested tissues after exposure to salinity stress; in contrast, the expression of two genes was significantly downregulated. The different expression patterns of HSP70 genes suggested that distinct response mechanisms might underlie HSP70-gene-related responses induced by specific environmental stressors. Similar results have also been reported in the spotted seabass. In analyses to measure the sensitivity of HSP70 genes in response to various environmental stresses, most of these genes exhibited highly inducible expression after heat stress; however, a large proportion of HSP70 genes showed significantly downregulated expression after hypoxia and alkalinity stress challenges [18]. In addition, two and four DE HSP70s were detected under low- and high-salinity conditions, respectively, in gills, demonstrating that HSP70 genes may have been more sensitive to high-salinity stress than to low-salinity stress. Furthermore, no DE HSP70 genes were found in the kidney or liver under either low- or high-salinity stress conditions, demonstrating obvious tissue-specific expression patterns of HSP70 genes under salinity stress conditions. Finally, we concluded that the expression of four HSP70 genes, *hsp70*, *hspa1b*, *hspa5*, and *hspa8a.1*, was significantly induced by both heat and salinity stress exposure, indicating their essential roles in participating in various abiotic stresses.

To determine the functions of HSP70 genes in participating in biotic stress, we investigated the expression patterns of HSP70 genes in the turbot after challenges with three different pathogens for the first time. The expression of 8, 10, and 9 DE HSP70 genes was detected after parasitic (*E. scophthalmi*), bacterial (*V. anguillarum*), and viral (*Megalocytivirus*) infection, respectively, and most of these genes showed significantly upregulated expression. Among these pathogen-activated genes, six genes (*hsp70*, *hspa1b*, *hspa4a*, *hspa4l*, *hspa5*, and *hspa9*) were differentially expressed under all three diverse pathogen infection stresses, suggesting their involvement in response to distinct biotic stresses. Nevertheless, different expression patterns of HSP70 genes were identified following infection with different pathogens. For example, DE *hsc70* were only detected after a challenge with *E. scophthalmi*, while DE *hspa13* was only identified after *V. anguillarum* infection. Otherwise, different numbers of DE HSP70 genes were also detected in the same tissue of turbot infected with the three different pathogens, that is, two, two, and nine DE HSP70 genes were identified in the kidney after *E. scophthalmi*, *V. anguillarum*, and *Megalocytivirus* infection, respectively. In the channel catfish, different expression patterns of HSP70 genes have also been detected after infection with *Flavobacterium columnare* and *Edwardsiella ictaluri* [14]. In addition, tissue-specific expression patterns have also been observed after these three pathogen infections; for instance, after *E. scophthalmi* infection, two, five, one, and two significantly

upregulated HSP70 genes were identified in the kidney, pyloric caeca, thymus, and blood, respectively, whereas no DE HSP70 genes were found in the spleen. Similarly, three, three, two, and seven HSP70 genes showed significantly up- or downregulated expression in the intestine, gill, kidney, and liver after infection with *V. anguillarum*, but no DE HSP70 genes were identified in the spleen. These results suggest that both pathogenesis-specific and tissue-specific expression patterns of HSP70 genes existed in the turbot.

4. Materials and Methods

4.1. Genome-Wide Identification and Sequence Analysis of HSP70 Genes in Turbot

To identify the full set of HSP70 genes in the turbot, the genome sequence, annotation file, and protein sequences of the turbot were first collected from NCBI databases (GCA_022379125.1) [33]. Then, two strategies were used to search the turbot genome to identify HSP70 genes. First, HSP70 protein sequences of the *Danio rerio* were used as a query database to search against turbot amino acid sequences using the BLASTp programs with default parameters. Second, a hidden Markov model (HMM) search using the HMM profile of the HSP70 domain (PF00012) derived from the Pfam protein family database and the HMM profiles of HSP12a and HSP12b (PTHR14187:SF46 and PTHR14187:SF39) retrieved from the PANTHER classification system as queries was conducted to identify candidate HSP70 proteins in the turbot genome using HMMER software (<https://www.ebi.ac.uk/Tools/hmmer/search/hmmsearch>, accessed on 1 August 2022) with an *E*-value of 10^{-4} . Next, the candidate protein sequences were submitted to the Conserved Domains Database (CDD) of NCBI to further confirm the presence of the conserved domains with an *E*-value of 10^{-4} . Next, the physicochemical properties of HSP70 proteins, including the MWs, number of amino acids, the theoretical isoelectric point (pI), GRAVY, and the II, were analyzed using the online ExPASy ProtParam tool.

4.2. Phylogenetic Analysis of the HSP70 Genes

To clarify the phylogenetic relationships and classification of HSP70 genes among different teleost species, the amino acid sequences of HSP70 genes from the turbot and other selected teleost species, such as the *D. rerio*, *Oryzias latipes*, and *Lepisosteus oculatus*, were employed to construct a phylogenetic tree. These protein sequences were downloaded from the NCBI and UniProt databases. Multiple protein sequence alignments were performed using the ClustalW method with default parameters in MEGA 11.0 [50]. Then, a neighbor-joining (NJ) phylogenetic tree was constructed by MEGA 11.0 software with the pairwise-deletion option based on the Jones–Taylor–Thornton (JTT) amino acid substitution model. A phylogenetic analysis was performed using the bootstrap method with 1000 replications to evaluate the support for the predicted phylogenetic relationships. Finally, EvolView (v2.0) (<https://www.evolgenius.info/evolview/>, accessed on 3 August 2022) was used to visualize the phylogenetic tree.

4.3. Chromosome Distribution and Molecular Evolution Analysis

To clarify the chromosomal distribution of HSP70 genes in the turbot genome, information on chromosome length and gene position was obtained from the genome Generic Feature Format (GFF) file, and then the genes were visualized using the gene location visualize function in TBtools (v1.098761) [51]. In addition, to determine the evolutionary constraints and selection pressure on HSP70 genes, the *K_a*, *K_s*, and *K_a/K_s* ratio of duplicated HSP70 gene pairs were calculated by the simple *K_a/K_s* calculator functions in TBtools.

4.4. Gene Structure Analysis and Conserved Motif Identification

The combination of the phylogenetic relationship and exon–intron structure of turbot HSP70 genes was visualized using the Gene Structure Display Server (GSDS, version 2.0, <http://gsds.cbi.pku.edu.cn>, accessed on 6 August 2022) with the genome GTF file and the phylogenetic tree file constructed by MEGA 11.0 as the input data. Furthermore, conserved

motif identification of the HSP70 proteins was performed using the online program MEME (5.4.1) [52] with the number of motifs set to 21 and the other parameters set to default.

4.5. Subcellular Localization and Protein Structure Prediction of HSP70

The subcellular localization of HSP70 proteins was detected by the online WoLF PSORT tool (<https://www.genscript.com/wolf-psort.html>, accessed on 8 August 2022). Then, the secondary structure of HSP70 proteins was predicted using online SOPMA software (http://npsa-pbil.ibcp.fr/cgi-bin/npsa_automat.pl?page=npsa_sopma.html, accessed on 8 August 2022). Signal peptides were predicted using the online SignalP 6.0 software (<https://services.healthtech.dtu.dk/service.php?SignalP>, accessed on 8 August 2022).

4.6. RNA-seq Datasets Used for the Expression Profiles of HSP70 Genes under Abiotic Stresses

Five published RNA-seq datasets related to abiotic stress (heat and salinity stress) (Table S8) were obtained from the NCBI SRA database to investigate the expression profiles of the HSP70 genes in the turbot under abiotic stresses. Specifically, two RNA-seq datasets were used for the expression analysis of the HSP70 genes after heat treatment. In the SRP152627 experiment, turbot individuals were exposed to heat stress (23 °C, 25 °C, and 28 °C). After heat treatment for 24 h, the kidney tissues in the turbot in the heat-treated groups and control group, which were maintained at 14 °C, were collected for RNA-seq [26]. In the SRA study of SRP273870, the liver tissues in the treatment groups exposed to heat stress (20 °C, 24 °C, and 28 °C) for 24 h and in the control group (14 °C) were used for RNA-seq [53]. For an expression analysis under salinity stress conditions, three salinity-stress-related RNA-seq datasets were collected. In the SRA study of SRP238143, the gill tissues of turbot after low-salinity (5‰), natural seawater (30‰), and high-salinity (50‰) treatments for 24 h were obtained for RNA-seq [28]. In SRP153594, the kidney tissues of turbot after different salinity (5‰, 30‰, and 50‰) treatments for 24 h were collected for RNA-seq. In SRP277001, the liver tissues of turbot subjected to freshwater (0‰) and natural seawater (30‰) were collected at 24 h and used for RNA-seq [27].

4.7. RNA-seq Datasets Used for the Expression Profiles of HSP70 Genes under Biotic Stresses

To investigate the expression patterns of the HSP70 genes in the turbot under biotic stress conditions, multiple pathogen-stress-related RNA-seq datasets after parasite (*Enteromyxum scophthalmi*), bacterial (*Vibrio anguillarum*), and viral (Megalocytivirus) challenges were retrieved from the NCBI SRA database (Table S8). For parasite infection stress, four RNA-seq datasets from 5 distinct tissues in healthy and *E. scophthalmi*-infected turbot were downloaded. In experiments SRP065375 and SRP050607, head kidney, spleen, and pyloric caeca tissues were collected for RNA-seq after challenges with *E. scophthalmi* for 24 and 42 days [31,34]. In the SRA study of SRP308109, blood samples collected from four levels of *E. scophthalmi*-infected (incipient, slight, moderate, and severe) turbot and from healthy turbot were used for RNA-seq [29]. In SRP255305, thymus tissues from healthy and infected turbot at 24 and 42 days post-infection with *E. scophthalmi* were selected for RNA-seq [35]. For bacterial challenge stress, data from five SRA studies were collected. In the SRA study of SRP191266, intestine tissues sampled at 0 h, 1 h, 4 h, and 12 h after infection with *V. anguillarum* were used for RNA-seq [30]. In SRA studies of SRP336094, SRP335896, SRP320422, and SRP319434, the liver, head kidney, gill and spleen tissues of turbot after a *V. anguillarum* challenge were collected for RNA-seq [32]. For viral infection, the SRA data from the SRP347383 study were downloaded. Specifically, head kidney tissues from healthy and infected turbot at 3, 6, and 9 days after infection with *Megalocytivirus* were collected for RNA-seq [54].

4.8. Expression Analyses of HSP70 Genes

To illustrate the expression patterns of HSP70 genes under biotic and abiotic stresses, the reads of the aforementioned stress-related RNA-seq datasets were first aligned to the turbot genome by STAR [55] with default parameters. Next, the featureCounts [56] software

program in Subread (v2.0.3) [57] was used to count the reads mapped to the genome to generate read count matrixes. With read count matrixes as inputs, edgeR [58] was used to identify differentially expressed (DE) (or significantly up- or downregulated) HSP70 genes based on the criteria of $|\log_2\text{fold change (FC)}| > 1$ and false discovery rate (FDR) < 0.01 . Moreover, transcripts per million (TPM) were calculated based on the read count matrixes. Finally, heatmaps showing the expression patterns of HSP70 genes were generated using TBtools (v1.098761) [51] with normalized TPM data ($\log_2(\text{TPM} + 1)$).

4.9. Heat Stress and *Edwardsiella Tarda* Challenge Experiment

In the heat stress experiment, 80 turbot individuals (26 ± 2.02 g) were randomly divided into four groups and acclimated at 18 °C for 7 days. Then, the water temperature was increased at a constant rate of 1 °C/h until it reached the desired experimental temperature (22 °C (T1), 26 °C (T2), and 30 °C (T3), and the control group (C) was maintained at 18 °C). After heat stress exposure for 24 h, three individuals per group were randomly sampled. Sampled fish were anesthetized with clove oil, and the liver and kidney tissues were collected and flash-frozen in liquid nitrogen and stored at -80 °C until RNA extraction.

In the *E. tarda* challenge experiment, 60 healthy turbot individuals (25 ± 2.45 g) were randomly divided into two groups, the control group and the *E. tarda* challenge group. *E. tarda* was cultured in lysogeny broth (LB) at 28 °C overnight for 24 h using a shaker incubator. In the challenge group, the fish were challenged by intraperitoneal injection with 100 μL of an *E. tarda* suspension consisting of 10^7 CFU/mL per 1 g body weight, while the fish in the control group were injected with the same volume of 1x PBS solution. At 0, 6, 12, 24, and 48 h post-injection (hpi), three individuals per group were randomly selected for kidney and spleen tissue collection. The sampling method was the same as that performed in the heat stress experiment.

4.10. Quantitative Real-Time PCR (qPCR)

To further validate the gene expression of the candidate HSP70 genes that responded to both biotic and abiotic stresses, qPCR was performed. The primers used to amplify the genes and β -actin (the internal control) were designed using Primer-BLAST of NCBI, and the sequences are listed in Table S9. qPCR assays were performed on a 7500 Fast Real-Time PCR System (ABI, Los Angeles, CA, USA) with THUNDERBIRD[®] Next SYBR[®] qPCR Mix (TOYOBO, Osaka, Japan). The construction of the qPCR system and the amplification conditions were carried out according to the instructions of the THUNDERBIRD[®] Next SYBR[®] qPCR Mix. The relative mRNA expression levels were calculated using the $2^{-\Delta\Delta\text{Ct}}$ method. Statistical analysis of the relative mRNA expression level was performed using one-way ANOVA with SPSS 26.0 (v26) software, and the differences were considered significant when the *p* value < 0.05 (*) and extremely significant when the *p* value < 0.01 (**).

5. Conclusions

Notably, through a comprehensive investigation of the expression profiles of HSP70 genes under abiotic and biotic stresses, *hsp70* (*hspa1a*), *hspa1b*, and *hspa5* showed significant responses to all five diverse stresses, heat, salinity, and *E. scophthalmi*, *V. anguillarum*, and *Megalocytivirus* infection stresses, indicating their potential roles in comprehensive anti-stress responses. To date, most of the previous studies on stress in teleosts have focused only on a single stress condition. In contrast, comprehensive study on multiple stress conditions has only been reported for the spotted seabass, which showed that *hsp70.2* was involved in the response to various environmental stresses (heat, alkalinity, and hypoxia stress) [18]. To further validate the functions of these three candidate comprehensive anti-stress HSP70 genes (*hsp70* (*hspa1a*), *hspa1b*, and *hspa5*), we conducted heat stress and *E. tarda* infection stress experiments and performed qPCR analysis. The results showed that the expression of *hsp70* (*hspa1a*), *hspa1b*, and *hspa5* was indeed significantly or extremely significant upregulated after heat and *E. tarda*-infection stresses, indicating the crucial roles of these genes in response to biotic and abiotic stresses.

Supplementary Materials: The supporting information can be downloaded at: <https://www.mdpi.com/article/10.3390/ijms24076025/s1>.

Author Contributions: Conceptualization, W.Z., X.X., S.C. and Y.L.; methodology, W.Z.; software, X.X.; validation, Y.C., W.Z., J.W., T.Z. and Z.E.; writing—original draft preparation, W.Z., X.X. and Y.C.; writing—review and editing, S.C. and Y.L.; funding acquisition, S.C. All authors have read and agreed to the published version of the manuscript.

Funding: This research was funded by the Fund of Special Scientific Research Funds for Central Non-profit Institutes, Yellow Sea Fisheries Research Institute (20603022021001), Central Public-interest Scientific Institution Basal Research Fund, CAFS (2020TD20), Shandong Key R&D Program (For Academician team in Shandong, 2023ZLYS02), and Taishan Scholar Climbing Project Fund of Shandong, China.

Institutional Review Board Statement: The animal study protocol was approved by the Institute Animal Care and Use committee, IACUC (protocol code YSFRI-2023004, on 1 January 2023).

Informed Consent Statement: Not applicable.

Data Availability Statement: The datasets analyzed for this study can be found in NCBI: <https://www.ncbi.nlm.nih.gov/> (accessed on 7 March 2022). The accession numbers can be found below: SRP152627, SRP273870, SRP277001, SRP238143, SRP153594, SRP308109, SRP255305, SRP065375, SRP050607, SRP191266, SRP336094, SRP335896, SRP320422, SRP319434, and SRP347383.

Acknowledgments: We thank the contributors for all the above published RNAseq datasets.

Conflicts of Interest: The authors declare no conflict of interest.

References

1. Ritossa, F.M. A new puffing pattern induced by temperature shock and DNP in drosophila. *Experientia* **1962**, *18*, 571–573. [[CrossRef](#)]
2. Feder, M.E.; Hofmann, G.E. Heat-shock proteins, molecular chaperones, and the stress response: Evolutionary and ecological physiology. *Annu. Rev. Physiol.* **1999**, *61*, 243–282. [[CrossRef](#)] [[PubMed](#)]
3. Kampinga, H.H.; Hageman, J.; Vos, M.J.; Kubota, H.; Tanguay, R.M.; Bruford, E.A.; Cheetham, M.E.; Chen, B.; Hightower, L.E. Guidelines for the nomenclature of the human heat shock proteins. *Cell Stress Chaperones* **2009**, *14*, 105–111. [[CrossRef](#)] [[PubMed](#)]
4. Hartl, F.U.; Bracher, A.; Hayer-Hartl, M. Molecular chaperones in protein folding and proteostasis. *Nature* **2011**, *475*, 324–332. [[CrossRef](#)]
5. Kiang, J.G.; Tsokos, G.C. Heat shock rotein 70 kDa molecular biology, biochemistry, and physiology. *Pharmacol. Ther.* **1998**, *80*, 183–201. [[CrossRef](#)]
6. Gupta, A.; Bansal, A.; Hashimoto-Torii, K. HSP70 and HSP90 in neurodegenerative diseases. *Neurosci. Lett.* **2020**, *716*, 134678. [[CrossRef](#)]
7. Daugaard, M.; Rohde, M.; Jaattela, M. The heat shock protein 70 family: Highly homologous proteins with overlapping and distinct functions. *FEBS Lett.* **2007**, *581*, 3702–3710. [[CrossRef](#)]
8. Boone, A.N.; Vijayan, M.M. Constitutive heat shock protein 70 (HSC70) expression in rainbow trout hepatocytes: Effect of heat shock and heavy metal exposure. *Comp. Biochem. Phys. C* **2002**, *132*, 223–233. [[CrossRef](#)]
9. Frydman, J. Folding of newly translated proteins in vivo: The role of molecular chaperones. *Annu. Rev. Biochem.* **2001**, *70*, 603–647. [[CrossRef](#)]
10. Ellis, J. Proteins as molecular chaperones. *Nature* **1987**, *328*, 378–379. [[CrossRef](#)]
11. Auluck, P.K.; Chan, H.Y.E.; Trojanowski, J.Q. Chaperone suppression of α -synuclein toxicity in a Drosophila model for Parkinson's disease. *Science* **2002**, *295*, 865–868. [[CrossRef](#)] [[PubMed](#)]
12. Moseley, P.L. Heat shock proteins and heat adaptation of the whole organism. *J. Appl. Physiol.* **1997**, *83*, 1413–1417. [[CrossRef](#)] [[PubMed](#)]
13. Shi, Q.; Yu, C.; Zhu, D.; Li, S.; Wen, X. Effects of dietary Sargassum horneri on resisting hypoxia stress, which changes blood biochemistry, antioxidant status, and hepatic HSP mRNA expressions of juvenile black sea bream *Acanthopagrus schlegelii*. *J. Appl. Phycol.* **2020**, *32*, 3457–3466. [[CrossRef](#)]
14. Song, L.; Li, C.; Xie, Y.; Liu, S.; Zhang, J.; Yao, J.; Jiang, C.; Li, Y.; Liu, Z. Genome-wide identification of Hsp70 genes in channel catfish and their regulated expression after bacterial infection. *Fish Shellfish. Immunol.* **2016**, *49*, 154–162. [[CrossRef](#)]
15. Deane, E.E.; Woo, N.Y.S. Impact of heavy metals and organochlorines on hsp70 and hsc70 gene expression in black sea bream fibroblasts. *Aquat. Toxicol.* **2006**, *79*, 9–15. [[CrossRef](#)]
16. Mosser, D.D.; Theodorakis, N.G.; Morimoto, R.I. Coordinate changes in heat shock element-binding activity and HSP70 gene transcription rates in human cells. *Mol. Cell. Biol.* **1988**, *8*, 4736–4744. [[CrossRef](#)]
17. Tsan, M.F.; Gao, B. Heat shock proteins and immune system. *J. Leukoc. Biol.* **2009**, *85*, 905–910. [[CrossRef](#)]

18. Sun, Y.; Wen, H.; Tian, Y.; Mao, X.; Li, X.; Li, J.; Hu, Y.; Liu, Y.; Li, J.; Li, Y. HSP90 and HSP70 families in *Lateolabrax maculatus*: Genome-wide identification, molecular characterization, and expression profiles in response to various environmental stressors. *Front. Physiol.* **2021**, *12*, 784803. [[CrossRef](#)]
19. Xu, K.; Xu, H.; Han, Z. Genome-wide identification of Hsp70 genes in the large yellow croaker (*Larimichthys crocea*) and their regulated expression under cold and heat stress. *Genes* **2018**, *9*, 590. [[CrossRef](#)]
20. Deng, Z.; Sun, S.; Gao, T.; Han, Z. The Hsp70 gene family in *Boleophthalmus pectinirostris*: Genome-wide identification and expression analysis under high ammonia stress. *Animals* **2019**, *9*, 36. [[CrossRef](#)]
21. Deng, Z.; Liu, H.; He, C.; Shou, C.; Han, Z. Heat shock protein 70 (Hsp70) and heat shock transcription factor (Hsf) gene families in *Cynoglossus semilaevis*: Genome-wide identification and correlation analysis in response to low salinity stress. *Mar. Freshw. Res.* **2021**, *72*, 1132–1141. [[CrossRef](#)]
22. Ma, F.; Luo, L. Genome-wide identification of Hsp70/110 genes in rainbow trout and their regulated expression in response to heat stress. *PeerJ* **2020**, *8*, e10022. [[CrossRef](#)] [[PubMed](#)]
23. Liu, K.; Hao, X.; Wang, Q.; Hou, J.; Lai, X.; Dong, Z.; Shao, C. Genome-wide identification and characterization of heat shock protein family 70 provides insight into its divergent functions on immune response and development of *Paralichthys olivaceus*. *PeerJ* **2019**, *7*, e7781. [[CrossRef](#)] [[PubMed](#)]
24. Bjørndal, T.; Øiestad, V. *The Development of a New Farmed Species: Production Technology and Markets for Turbot*; Working Paper; Institute for Research in Economics and Business Administration: Bergen, Norway, 2010.
25. Lei, J.L.; Liu, X.F.; Guan, C.T. Turbot culture in China for two decades: Achievements and prospect. *Prog. Fish. Sci.* **2012**, *33*, 123–130. [[CrossRef](#)]
26. Huang, Z.; Ma, A.; Yang, S.; Liu, X.; Zhao, T.; Zhang, J.; Wang, X.A.; Sun, Z.; Liu, Z.; Xu, R. Transcriptome analysis and weighted gene co-expression network reveals potential genes responses to heat stress in turbot *Scophthalmus maximus*. *Comp. Biochem. Physiol. D-Genom. Proteom.* **2020**, *33*, 100632. [[CrossRef](#)]
27. Liu, Z.; Ma, A.; Yuan, C.; Zhao, T.; Chang, H.; Zhang, J. Transcriptome analysis of liver lipid metabolism disorders of the turbot *Scophthalmus maximus* in response to low salinity stress. *Aquaculture* **2021**, *534*, 736273. [[CrossRef](#)]
28. Cui, W.; Ma, A.; Huang, Z.; Wang, X.a.; Sun, Z.; Liu, Z.; Zhang, W.; Yang, J.; Zhang, J.; Qu, J. Transcriptomic analysis reveals putative osmoregulation mechanisms in the kidney of euryhaline turbot *Scophthalmus maximus* responded to hypo-saline seawater. *J. Oceanol. Limnol.* **2019**, *38*, 467–479. [[CrossRef](#)]
29. Ronza, P.; Alvarez-Dios, J.A.; Robledo, D.; Losada, A.P.; Romero, R.; Bermudez, R.; Pardo, B.G.; Martinez, P.; Quiroga, M.I. Blood transcriptomics of turbot *Scophthalmus maximus*: A tool for health monitoring and disease studies. *Animals* **2021**, *11*, 1296. [[CrossRef](#)]
30. Gao, C.; Cai, X.; Cao, M.; Fu, Q.; Yang, N.; Liu, X.; Wang, B.; Li, C. Comparative analysis of the miRNA-mRNA regulation networks in turbot (*Scophthalmus maximus* L.) following *Vibrio anguillarum* infection. *Dev. Comp. Immunol.* **2021**, *124*, 104164. [[CrossRef](#)]
31. Ronza, P.; Robledo, D.; Bermudez, R.; Losada, A.P.; Pardo, B.G.; Sitja-Bobadilla, A.; Quiroga, M.I.; Martinez, P. RNA-seq analysis of early enteromyxosis in turbot (*Scophthalmus maximus*): New insights into parasite invasion and immune evasion strategies. *Int. J. Parasitol.* **2016**, *46*, 507–517. [[CrossRef](#)]
32. Song, Y.; Dong, X.; Hu, G. Transcriptome analysis of turbot (*Scophthalmus maximus*) head kidney and liver reveals immune mechanism in response to *Vibrio anguillarum* infection. *J. Fish Dis.* **2022**, *45*, 1045–1057. [[CrossRef](#)] [[PubMed](#)]
33. Xu, X.-w.; Zheng, W.; Meng, Z.; Xu, W.; Liu, Y.; Chen, S. Identification of stress-related genes by co-expression network analysis based on the improved turbot genome. *Sci. Data* **2022**, *9*, 374. [[CrossRef](#)] [[PubMed](#)]
34. Robledo, D.; Ronza, P.; Harrison, P.W.; Losada, A.P.; Bermudez, R.; Pardo, B.G.; Redondo, M.J.; Sitja-Bobadilla, A.; Quiroga, M.I.; Martinez, P. RNA-seq analysis reveals significant transcriptome changes in turbot (*Scophthalmus maximus*) suffering severe enteromyxosis. *BMC Genom.* **2014**, *15*, 1149. [[CrossRef](#)] [[PubMed](#)]
35. Ronza, P.; Robledo, D.; Losada, A.P.; Bermudez, R.; Pardo, B.G.; Martinez, P.; Quiroga, M.I. The teleost thymus in health and disease: New insights from transcriptomic and histopathological analyses of turbot, *Scophthalmus maximus*. *Biology* **2020**, *9*, 221. [[CrossRef](#)]
36. Rosenzweig, R.; Nillegoda, N.B.; Mayer, M.P.; Bukau, B. The Hsp70 chaperone network. *Nat. Rev. Mol. Cell Biol.* **2019**, *20*, 665–680. [[CrossRef](#)]
37. Karlin, S.; Brocchieri, L. Heat shock protein 70 family: Multiple sequence comparisons, function, and evolution. *J. Mol. Evol.* **1998**, *47*, 565–577. [[CrossRef](#)]
38. Gao, L.; Yuan, Z.; Yu, S.; Yang, Y.; Li, Y.; He, C. Genome-wide identification of HSP70/110 genes in sea cucumber *Apostichopus japonicus* and comparative analysis of their involvement in aestivation. *Comp. Biochem. Physiol. D-Genom. Proteom.* **2018**, *28*, 162–171. [[CrossRef](#)]
39. Hu, Z.; Song, H.; Feng, J.; Zhou, C.; Yang, M.-J.; Shi, P.; Yu, Z.-L.; Li, Y.-R.; Guo, Y.-J.; Li, H.-Z.; et al. Massive heat shock protein 70 genes expansion and transcriptional signatures uncover hard clam adaptations to heat and hypoxia. *Front. Mar. Sci.* **2022**, *9*, 898669. [[CrossRef](#)]
40. Jin, S.; Deng, Z.; Xu, S.; Zhang, H.; Han, Z. Genome-wide identification and low-salinity stress analysis of the Hsp70 gene family in swimming crab (*Portunus trituberculatus*). *Int. J. Biol. Macromol.* **2022**, *208*, 126–135. [[CrossRef](#)]

41. Zhang, G.; Fang, X.; Guo, X.; Li, L.; Luo, R.; Xu, F.; Yang, P.; Zhang, L.; Wang, X.; Qi, H.; et al. The oyster genome reveals stress adaptation and complexity of shell formation. *Nature* **2012**, *490*, 49–54. [[CrossRef](#)]
42. Brocchieri, L.; de Macario, E.C.; Macario, A.J.L. hsp70 genes in the human genome: Conservation and differentiation patterns predict a wide array of overlapping and specialized functions. *BMC Evol. Biol.* **2008**, *8*, 19. [[CrossRef](#)] [[PubMed](#)]
43. Moore, R.C.; Purugganan, M.D. The early stages of duplicate gene evolution. *Proc. Natl. Acad. Sci. U.S.A.* **2003**, *100*, 15682–15687. [[CrossRef](#)] [[PubMed](#)]
44. Kong, H.; Landherr, L.L.; Frohlich, M.W.; Leebens-Mack, J.; Ma, H.; dePamphilis, C.W. Patterns of gene duplication in the plant SKP1 gene family in angiosperms: Evidence for multiple mechanisms of rapid gene birth. *Plant J.* **2007**, *50*, 873–885. [[CrossRef](#)] [[PubMed](#)]
45. Voldoire, E.; Brunet, F.; Naville, M.; Volff, J.-N.; Galiana, D. Expansion by whole genome duplication and evolution of the sox gene family in teleost fish. *PLoS ONE* **2017**, *12*, e0180936. [[CrossRef](#)] [[PubMed](#)]
46. Holub, E.B. The arms race is ancient history in Arabidopsis, the wildflower. *Nat. Rev. Genet.* **2001**, *2*, 516–527. [[CrossRef](#)]
47. Wang, J.; Pan, C.; Wang, Y.; Ye, L.; Wu, J.; Chen, L.; Zou, T.; Lu, G. Genome-wide identification of MAPK, MAPKK, and MAPKKK gene families and transcriptional profiling analysis during development and stress response in cucumber. *BMC Genom.* **2015**, *16*, 386. [[CrossRef](#)]
48. Zhang, J.; Li, J.; Liu, B.; Zhang, L.; Chen, J.; Lu, M. Genome-wide analysis of the Populus Hsp90 gene family reveals differential expression patterns, localization, and heat stress responses. *BMC Genom.* **2013**, *14*, 532. [[CrossRef](#)]
49. Huang, X.; Li, S.; Gao, Y.; Zhan, A. Genome-wide identification, characterization and expression analyses of heat shock protein-related genes in a highly invasive ascidian *Ciona savignyi*. *Front. Physiol.* **2018**, *9*, 1043. [[CrossRef](#)]
50. Tamura, K.; Stecher, G.; Kumar, S. MEGA11: Molecular evolutionary genetics analysis version 11. *Mol. Biol. Evol.* **2021**, *38*, 3022–3027. [[CrossRef](#)]
51. Chen, C.; Chen, H.; Zhang, Y.; Thomas, H.R.; Frank, M.H.; He, Y.; Xia, R. TBtools: An integrative toolkit developed for interactive analyses of big biological data. *Mol. Plant* **2020**, *13*, 1194–1202. [[CrossRef](#)]
52. Bailey, T.L.; Johnson, J.; Grant, C.E.; Noble, W.S. The MEME Suite. *Nucleic Acids Res.* **2015**, *43*, W39–W49. [[CrossRef](#)] [[PubMed](#)]
53. Zhao, T.; Ma, A.; Huang, Z.; Liu, Z.; Sun, Z.; Zhu, C.; Yang, J.; Li, Y.; Wang, Q.; Qiao, X.; et al. Transcriptome analysis reveals that high temperatures alter modes of lipid metabolism in juvenile turbot (*Scophthalmus maximus*) liver. *Comp. Biochem. Physiol. D-Genom. Proteom.* **2021**, *40*, 100887. [[CrossRef](#)] [[PubMed](#)]
54. Xu, X.; Liu, L.; Feng, J.; Li, X.; Zhang, J. Comparative transcriptome analysis reveals potential anti-viral immune pathways of turbot (*Scophthalmus maximus*) subverted by megalocytivirus RBIV-C1 for immune evasion. *Fish Shellfish. Immunol.* **2022**, *122*, 153–161. [[CrossRef](#)] [[PubMed](#)]
55. Dobin, A.; Davis, C.A.; Schlesinger, F.; Drenkow, J.; Zaleski, C.; Jha, S.; Batut, P.; Chaisson, M.; Gingeras, T.R. STAR: Ultrafast universal RNA-seq aligner. *Bioinformatics* **2013**, *29*, 15–21. [[CrossRef](#)]
56. Liao, Y.; Smyth, G.K.; Shi, W. featureCounts: An efficient general purpose program for assigning sequence reads to genomic features. *Bioinformatics* **2014**, *30*, 923–930. [[CrossRef](#)]
57. Liao, Y.; Smyth, G.K.; Shi, W. The Subread aligner: Fast, accurate and scalable read mapping by seed-and-vote. *Nucleic Acids Res.* **2013**, *41*, e108. [[CrossRef](#)]
58. Robinson, M.D.; McCarthy, D.J.; Smyth, G.K. edgeR: A Bioconductor package for differential expression analysis of digital gene expression data. *Bioinformatics* **2010**, *26*, 139–140. [[CrossRef](#)]

Disclaimer/Publisher’s Note: The statements, opinions and data contained in all publications are solely those of the individual author(s) and contributor(s) and not of MDPI and/or the editor(s). MDPI and/or the editor(s) disclaim responsibility for any injury to people or property resulting from any ideas, methods, instructions or products referred to in the content.